



Influence of humidity and temperature on the drying kinetics, phase composition and morphology of gypsum

M. Schwotzer¹, S.J. Ahmed², P. Iacomi², P.G. Weidler¹

Institute for functional Interfaces (IFG) Karlsruhe Institute of Technology (KIT)¹, Surface Measurement Systems Ltd².

Gypsum dehydration is a commonplace industrial process, which follows a complex mechanism spanning multiple phase transformations. With the help of the DVS Vacuum, it was possible to investigate the influence of relative humidity on the dehydration of gypsum in a temperature range between 25 °C and 60 °C. The mass loss observed by DVS was indicative of the formation of dehydrated phases, as confirmed through XRD Rietveld refinement. Through the subsequent observation of microstructure by SEM, the sample morphology evolution and insight into the vapor transport mechanism during degradation could be ascertained. Water activity is therefore an important parameter in the complex phase evolution of gypsum dehydration.

Introduction

The historical horizon of gypsum-based binder technology spans at least 11,000 years and ranges from building materials, ceramics, medical and food use alongside many industrial applications. The mineral gypsum, $\text{CaSO}_4 \cdot 2\text{H}_2\text{O}$, serves as the raw material for such compounds. To produce the starting materials or binders, gypsum is usually thermally converted into the phase bassanite (or plaster of Paris), $\text{CaSO}_4 \cdot 0.5\text{H}_2\text{O}$, or the water-soluble anhydrite, $\text{CaSO}_4 \cdot n\text{H}_2\text{O}$, $n < 0.05$. Due to its technical importance, the thermal behavior of the hydrate phases in the $\text{CaSO}_4 - \text{H}_2\text{O}$ system has been the subject of scientific activities for thousands of years [1]. For instance, details of the process control in binder production, such as the use of steam, were already described hundreds of years ago and discussed as state of the art [2]. However, the mechanisms of the processes that take place when gypsum is exposed to elevated temperatures are still the subject of intensive research activities and remain controversial [3, 4].

In this context, it is becoming increasingly clear that, in addition to the temperature applied, the humidity adjacent to the material plays a decisive

role both for the manufacturing processes of gypsum-based binders and for the stability and durability of the materials produced from them. Thus, the phase transformations in the $\text{CaSO}_4 - \text{H}_2\text{O}$ system through dissolution and recrystallization are expected to take place in aqueous thin films on the particle surfaces [5]. Here it becomes apparent that the key to understanding the mechanisms of these phase transformations must lie in the detailed knowledge about the extent and effect of water adsorbed on crystal surfaces. Moreover, from an economic perspective, control of humidity during the drying process has significant cost implications.

In this study, an extensive series of experiments were carried out to evaluate the influence of temperature and relative humidity on gypsum drying and the resulting phase composition and particle morphology. This was possible by monitoring the desorption kinetics at controlled humidity and temperature, carried out with a Dynamic Vapor Sorption (DVS) instrument, with the phase composition and morphology then were investigated using X-ray diffraction (XRD) and scanning electron microscopy (SEM).



Methods

The basic material was a gypsum or $\text{CaSO}_4 \cdot 2\text{H}_2\text{O}$ (CAS 10101-4104) obtained from VWR, Germany.

Drying at controlled humidity and temperature was monitored *in-situ* using a DVS Vacuum instrument. During the experiments an average 47.6 ± 10.8 mg of sample material was used. The duration of the measurement was between 142 hours and 18 hours, as the sample was dried until a complete weight equilibrium was achieved, depending on the applied temperature, which comprised steps of 25, 30, 40 and 60 °C. The relative humidity (RH) at the corresponding temperature was set to 0, 2.5 and 5.0%. The procedure consisted of a single step in which the mass loss was recorded every 20 seconds. The data stored in an Excel-file was then analyzed to yield weight-loss over time reported as a percentage of the initial sample mass.

XRD measurements were carried out on a Bruker AXS D8 Advance equipped with a Lynxeye® position sensitive detector in θ - θ geometry. A variable divergence slit was used on the source side with a 2.3° Soller-slit on the detector side. The XRD data was acquired over a 2θ range from 5° to 65°, with an acquisition time of 384 s per 0.02 ° 2θ -step. Total measurement time was 99 minutes. Data reduction and evaluation was done with in TOPAS 6.0 [6]. Structure files for the mineral's phases used in the Rietveld refinement were gypsum $\text{CaSO}_4 \cdot 2\text{H}_2\text{O}$, two bassanite or hemihydrate $\text{CaSO}_4 \cdot 1.8 \text{H}_2\text{O}$ and $\text{CaSO}_4 \cdot 0.6 \text{H}_2\text{O}$, the water-soluble γ -anhydrite CaSO_4 , and the water insoluble β -anhydrite CaSO_4 . All these structures were retrieved from the ICSD-FIZ [7] Diffractograms were obtained from the end products immediately after the DVS run was finished. The powder sample from the DVS was placed on a PMMA sample holder and flattened.

SEM experiments were carried out using an ESEM Quattro S from Thermo Fisher Scientific. The respective measurement conditions are shown in each image.

Results and Discussion

DVS Drying

The weight-loss over time at various temperature and relative humidity values is depicted in Figure 1. From the weight loss curves obtained by DVS it is evident that the humidity has an important influence on the dehydration process. The time to weight equilibrium shortens drastically with relative humidity. In addition, the influence of temperature also enhances the dehydration kinetics of gypsum.

Unsurprisingly, the weight loss is faster at lower ambient relative humidity and at higher temperatures. Whenever weight equilibrium was achieved the relative mass loss amounts to

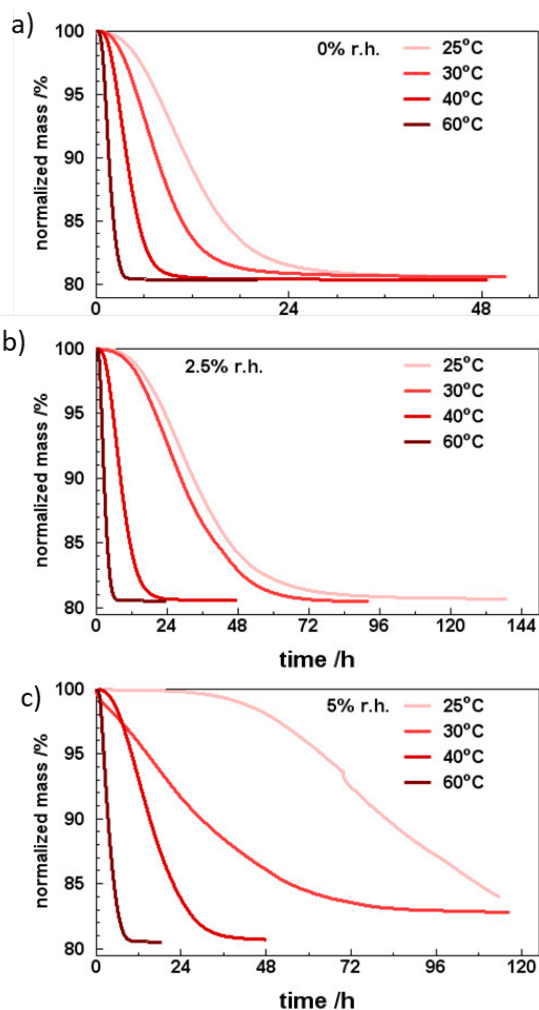


Figure 1. Relative change of mass over time for different relative humidity- and temperature values a) 0% RH b) 2.5% RH c) 5% RH



Table 1: Relative maximal mass loss at different temperature and corresponding relative humidity (RH)

	0% RH	2.5% RH	5.0% RH
Temperature (°C)	relative mass loss (%)	relative mass loss (%)	relative mass loss (%)
25	19.4	19.4	16.0
30	19.2	19.5	17.3
40	19.6	19.4	19.3
60	19.6	16.5	19.5

approximately 19.4% for relative humidity values of 0 and 2.5%, as summarized in Table 1.

The initial mineral phase can be assumed to be gypsum $\text{CaSO}_4 \cdot 2\text{H}_2\text{O}$, which can transform during the treatment into bassanite (hemihydrate) with different amounts of water, per unit formula, $\text{CaSO}_4 \cdot 1.8 \text{H}_2\text{O}$ and $\text{CaSO}_4 \cdot 0.6 \text{H}_2\text{O}$, and finally to a nearly dry water soluble γ -anhydrite $\text{CaSO}_4 \cdot n\text{H}_2\text{O}$, $n < 0.05$ then to a fully dry insoluble β -anhydrite CaSO_4 .

The mass loss observed in DVS is close to, but not exactly the stoichiometric value of 20.9% that corresponds to the departure of both coordinated water molecules from the crystal structure, which would result in a full dehydration and an β -anhydrite phase. Instead, mass loss is consistent to a stoichiometric ratio of $\text{CaSO}_4 \cdot 0.15 \text{H}_2\text{O}$. At a higher water vapor activity of 5% RH, dehydration was only achieved at temperatures over 40 °C while at lower temperatures full equilibrium was not achieved and correspondingly less mass was lost.

Phase Analysis

More in-depth phase analysis can be performed through XRD. The Rietveld refinement of the diffractograms using the above-mentioned phases yielded reliable results. In Figure 2 two example diffractograms of DVS dried samples are depicted. The mineral composition determined by refinement for all experiments is given in Figure 3.

The dominating mineral phase after activation was γ - CaSO_4 , followed by the bassanite containing 1.8 water molecules per units' formula, $\text{CaSO}_4 \cdot 1.8 \text{H}_2\text{O}$. The water insoluble β -anhydrite was not detected in any of the resulting phases. Gypsum, $\text{CaSO}_4 \cdot 2 \text{H}_2\text{O}$, was not found in most of the end products, except in those runs where the equilibrium of the

mass was not achieved due to time limitation. The "classical" hemihydrate, the bassanite containing 1/2 water, i.e. $\text{CaSO}_4 \cdot 0.5 \text{H}_2\text{O}$, played a minor role. Noteworthy, that the best Rietveld-fit for the hemihydrate was obtained by a mixture of the two bassanite structures consisting of 1.8 and 0.6 molecules of water in their structure.

On average the weight loss, as determined by the DVS, could be recalculated by the mineralogical composition of the end products expressed as the mass ratio by XRD to DVS within 100 +/- 6%.

The weight loss recalculated from the mineral composition determined by XRD analysis matched very well with the one measured by the DVS. This indicates the correctness of the number and kind of model structures applied for Rietveld refinement.

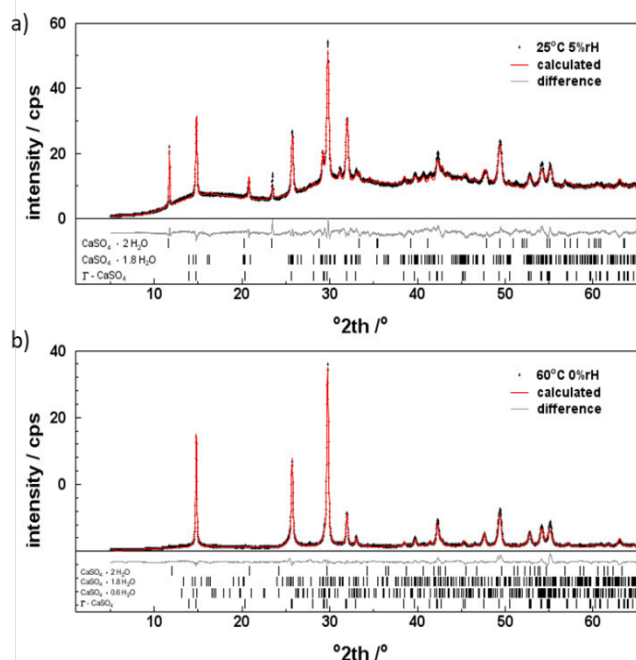


Figure 2. Diffractograms of samples treated a) 25 °C and 5.0% RH: b) 60 °C and 0% RH. Crosses denote measured data, red line the calculated pattern, gray line the difference between observation and calculation; vertical bars indicate peak position of the respective mineral phases.

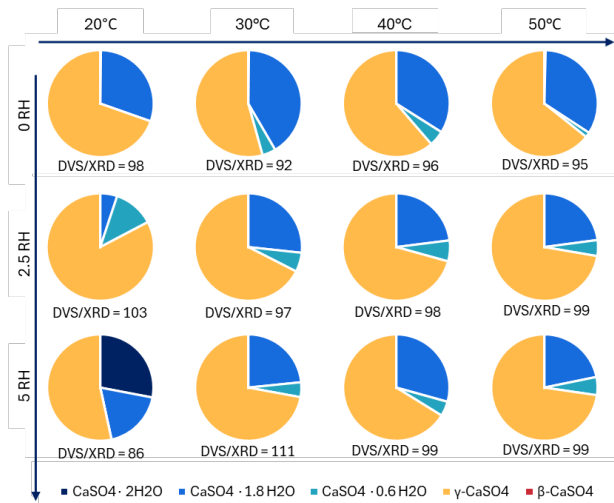


Figure 3 Mineralogical composition of the end products. All values in weight-%. n.d. not detected; XRD/DVS mass ratio of calculated mass (by XRD) and measured mass (by DVS).

Morphology Analysis

The original, untreated gypsum sample contains large crystals with smooth faces corresponding to the crystal system of gypsum (Figure 4a). The large flat faces can be attributed to the (010) face, whereas the edge consists of (011), (120) or (111) faces. Heating at 25 °C under the three applied relative humidity values resulted in more corrugated surfaces of the (010) faces. The SEM examinations reveal that although the particles retain their original shape after the reaction, they are interspersed with a network of cracks. In the enlarged sections of the samples after exposure at 0% RH, 2.5% RH and 5% RH, it can be seen that layer

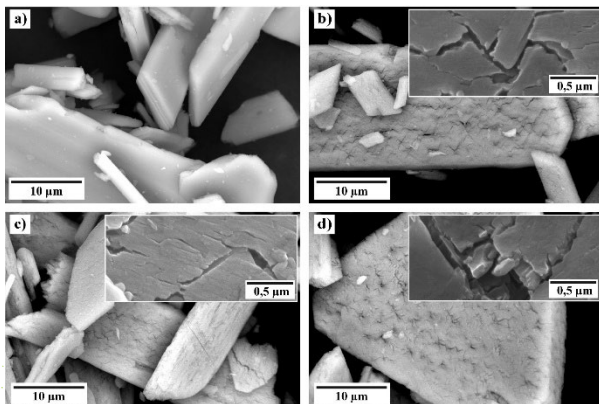


Figure 4. SEM images of the original gypsum (a) After exposure at 25 °C to 0% RH (b), 2.5% RH (c), 5% RH (d) with a close-up view (top right)

packages detach from the surface. These layers themselves consist of smaller, rod-shaped units, as shown in the detail enlargements in the insets of the Figures 4b-d.

It is remarkable that the original particle shape with the habitus which is typical for the starting material gypsum is retained, although - as shown in the XRD analysis - complex phase transformations take place. The surfaces of the (010) faces of particles are crisscrossed by a network of cracks. The appearance of the cracks can be explained by the transformation of gypsum into phases with a semi-hydrate structure. These phases have a lower molar volume (29% less). As the particle shape is retained, but the molar volume of the solid phases is reduced, stress builds up which in turn leads to the formation of cracks. For the further course of the dehydration reaction, the cracks in the crystal surfaces are considered to be escape channels for the water vapor produced during the dehydration of the gypsum. Okhotinikov report on observations made on gypsum surfaces, where water diffusion along [010] and [001] directions was investigated, which support this view [8]. In the context of this study, it seems appropriate to understand the crack system not only as a means of transporting the water released during the reaction. Throughout the pore system RH is expected to have different local values. Thus, within individual crystals the transformation will exhibit different rates. This behavior is reflected in the variation of the mineral composition as determined by XRD

Kinetic Analysis

From experiments at the 4 temperatures, the linear part of the mass loss curves yields the rate of the mass loss over time in mg/min. This slope, plotted in a logarithmic form over the inverse of temperature $1/T$ in Kelvin – an Arrhenius-plot see Figure 4 – allows the calculation of the activation energy E_A in kJ/mol. The values for E_A are presented in Table 2.

This value is close to the range of 84–97 kJ mol⁻¹ reported in literature for this complete gypsum dehydration process [10-12]. El Hazzat et. al found



higher E_A -Values of $96.03 \pm 1.89 \text{ kJ mol}^{-1}$ for the complete transformation of gypsum into bassanite at temperature between $130 \text{ }^\circ\text{C}$ and $180 \text{ }^\circ\text{C}$ with thermal gravimetry [9]. For the further reduction of the water content, bassanite to $\gamma\text{-CaSO}_4$, a second dehydration step and the corresponding activation energy of $80.63 \pm 2.21 \text{ kJ mol}^{-1}$ was also reported by El Hazzat et al. [9]. No values for the relative humidity were reported.

Table 2: Activation energy E_A at different RH

RH (%)	0	2.5	5.0
	kJ/mol	kJ/mol	kJ/mol
E_A	49.5	59.5	68.9
$E_A/E_A(0)$ normalized (%)	100	120	139

From Figure 5, the dependency of the activation energy on the surrounding relative humidity is evident. The higher the relative humidity the more energy in form of heat must be applied to the sample material in order to cause the water release and thus induce the structural transformation, which can be detected by XRD.

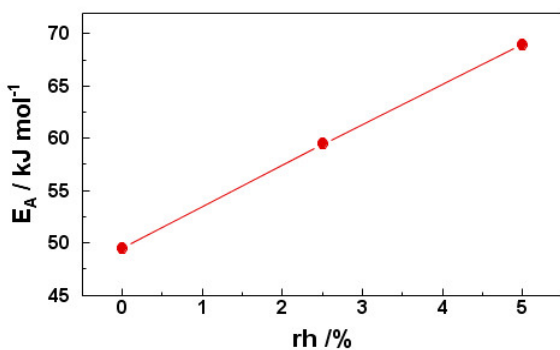


Figure 6. Activation energy as a function of ambient relative humidity

From the above findings the influence of the humidity in the gas phase is evident for the gypsum dehydration process. The higher the relative humidity the more thermal energy is needed to remove water from the samples. Or, on the contrary, the temperature needed for the dehydration can be lowered by reducing the water

activity in the surrounding gas phase, i.e. relative humidity, but at the cost of the duration of the transformation. This influence was proposed by Krause et al. and is now confirmed [5]. Still more experiments are needed because the water activity in the newly by dehydration created pores is expected to be different than outside the crystals. Thus, the dehydration at the pore walls, the release of water into the pore volume and its subsequent transport through this pore volume into the external gas phase will be the rate determining step. No allowance has herein been made towards phase transformation induced temperature effects, such as sample cooling, which may chance the

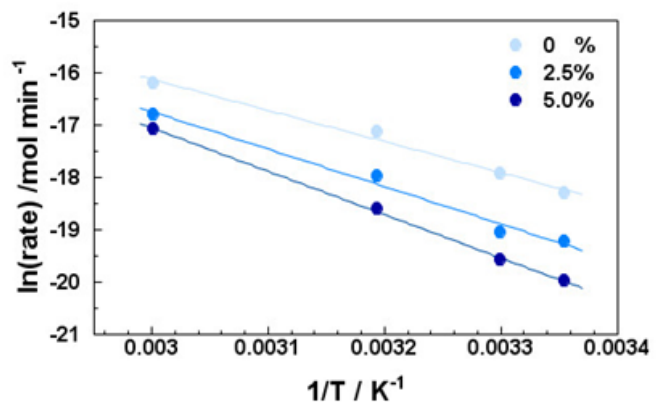


Figure 5. Rate of mass loss over time plotted over $1/T$ for the calculation of the activation energy E_A .

effective temperature of the transformation.

Conclusion

With the help of the DVS instrument, it was possible to investigate the influence of temperature and relative humidity on the dehydration kinetics of gypsum at temperatures between $25 \text{ }^\circ\text{C}$ and $60 \text{ }^\circ\text{C}$. The instrument showed great stability over a period of 6 days. The mass loss observed by DVS could be explained by the formation of the newly generated minerals as determined through XRD Rietveld refinement. Through the subsequent observation of microstructure by SEM, the sample morphology evolution and insight into the vapor transport mechanism during degradation could be ascertained. It can be concluded that water activity is an important parameter in the complex phase



evolution of the gypsum - bassanite - anhydrite transformation.

References

- [1] Stark, J.; Wicht, B. The history of gypsum and gypsum plaster. *ZKG Int.* **1999**, *52*, 527–533.
- [2] Hartmann, C. Die Kalk- und Gyps-Brennerei so wie die Mörtel- und Stuck-Bereitung nach ihrem neuesten Standpunkte; Verlag Gottfr. Basse: Quedlinburg/Leipzig, Germany, 1850.
- [3] Freyer, D.; Voigt, W. Crystallization and Phase Stability of CaSO_4 and CaSO_4 -Based Salts. *Monatsh. Chem.* **2003**, *134*, 693–719
- [4] Tang, Y.; Gao, J.; Liu, C.; Chen, X.; Zhao, Y. Dehydration Pathways of Gypsum and the Rehydration Mechanism of Soluble Anhydrite γ - CaSO_4 . *ACS Omega* **2019**, *4*, 7636–7642.
- [5] Krause, F.; Renner, B.; Coppens, F.; Dewanckele, J.; Schwotzer, M. Reactivity of Gypsum-Based Materials Subjected to Thermal Load: Investigation of Reaction Mechanisms. *Materials* **2020**, *13*, 1427.
- [6] Bruker AXS (2007) TOPAS V6: General profile and structure analysis software for powder diffraction data. - User's Manual, Bruker AXS, Karlsruhe, Germany
- [7] Inorganic crystal structure database (ICSD) <https://icsd.fiz-karlsruhe.de/index.xhtml>
- [8] Okhotnikov V.B., Petrov S.E., Yakobson B.I. and Lyakhov N.Z. (1987) dehydration of calcium sulphate dihydrate single crystals, *Reactivity of Solids* *2*, 359-372
- [9] El Hazzat M, Sifou A., Arsalane S. and El Hamidi A. (2020) Novel approach to thermal degradation kinetics of gypsum: application of peak deconvolution and Model-Free isoconversional method, *J. Thermal Analysis and Calorimetry* *140*, 657-671
- [10] Fukami T, Tahara S, Nakasone K, Yasuda C. Synthesis, crystal structure, and thermal properties of $\text{CaSO}_4 \cdot 2\text{H}_2\text{O}$ single crystals. *Int J Chem.* **2015**;15:12–20.
- [11] López-Beceiro J, Gracia-Fernández C, Tarrío-Saavedra J, Gómez-Barreiro S, Artiaga R. Study of gypsum by PDSC. *J Therm Anal Calorim.* **2012**;109:1177–83.
- [12] Sarma LP, Prasad PSR, Ravikumar N. Raman spectroscopic study of phase transitions in natural gypsum. *J Raman Spectrosc.* **1998**;29:851–6